On-Chip Vacuum Generated by a Micromachined Knudsen Pump

Shamus McNamara, *Member, IEEE,* and Yogesh B. Gianchandani, *Senior Member, IEEE*

***Abstract*—This paper describes the design, fabrication, and testing of a single-chip micromachined implementation of a Knudsen pump, which uses the principle of thermal transpiration, and has no moving parts. A six-mask microfabrication process was used to fabricate the pump using a glass substrate and silicon wafer. The Knudsen pump and two integrated pressure sensors occupy an area of 1.5 mm $\times$ 2 mm. Measurements show that while operating in standard laboratory conditions this device can evacuate a cavity to 0.46 atm using 80 mW input power. The pumpdown time of an on-chip chamber and pressure sensor cavity with a total volume of 80 000 cubic micrometers is only 2 s, with a peak pump speed of 1×10^{-6} cc/min. High thermal isolation is obtained between the polysilicon heater and the rest of the device. [1073]**

***Index Terms*—High temperature, thermal isolation, thermal transpiration, thermomolecular, vacuum pump.**

I. Introduction

MICROMACHINED gas pumps have a variety of potential applications, ranging from actuation of gases for gas chromatography, spectroscopy [1], or microplasma manufacturing [2], [3], to the pneumatic actuation of liquids for lab-on-a-chip and chemical sensing devices [4]. Conventional vacuum pumps scale down poorly due to increased surface to volume ratio and have reliability concerns due to the relative increase of frictional forces over inertial forces at the microscale. Thermal molecular pumps can potentially overcome these challenges.

There are three types of thermal molecular pumps [5]: the Knudsen pump [6], accommodation pump [7], and the thermomolecular pump [8]. The Knudsen pump relies upon the principle of thermal transpiration. Different temperatures are applied to two chambers at either end of a narrow tube. A net gas flow from the colder chamber to the hotter chamber occurs because of the temperature dependence of molecular flux rates through a narrow tube. The accommodation pump uses a similar geometry to the Knudsen pump, but the narrow tube is replaced with a smooth, wide tube. A net flow of gas occurs from the hot chamber to the cold chamber because the hot gas molecules have a greater chance of reflecting off the tube surface due to the higher tangential momentum accommodation coefficient (TMAC) of hot gas molecules. The thermomolecular pump exploits some materials that violate the cosine scattering law when heated. By positioning a material that emits a flux of gas with a larger flow perpendicular to its surface than the cosine scatter law would dictate, a net flow of gas will flow through the aperture.

The Knudsen pump was chosen in this effort[1] because it provides the highest compression ratio and, unlike the other two pumps, its performance is independent of the material and surface conditions, which can be difficult to characterize and control. A miniaturized Knudsen pump also has a high theoretical efficiency when compared to conventional vacuum pumps [11] and scales well to small dimensions because the efficiency improves as the surface to volume ratio increases. It offers potentially high reliability because there are no moving parts, but power consumption can be a major concern because of the elevated temperatures required. Recent developments in micromachining technology facilitate high thermal isolation and motivate a fresh look at this problem.

The Knudsen pump was first reported in 1910 and since then has been reported approximately once per decade [12]. Despite its attractive features, persistent challenges that have prevented its widespread adoption include the need for submicron dimensions to operate at atmosphere (and consequently it was always confined to high vacuum operation over a limited pressure range) and low throughput. The past decade has witnessed greater activity, with simulation efforts [13], [14] and a partially micromachined implementation achieving a best-case pressure drop of 11.5 torr using helium [15], [16].

This paper describes a single-chip micromachined Knudsen pump. The theory of operation of the Knudsen pump is described in Section II, followed by a description of the process used to fabricate the Knudsen pump in Section III. The measured results obtained from fabricated devices are reported in Section IV.

II. Knudsen Pump Theory

The principle of thermal transpiration [17], on which the Knudsen pump is based, describes the pressure-temperature relationship between two adjacent volumes of gas at different temperatures. If these two volumes of gas are separated by a channel or aperture that permits gas flow only in the free molecular regime (Fig. 1), they settle at different pressures, the ratio of which is a function of only temperature. The temperature

Manuscript received June 24, 2003; revised November 2, 2004. This work was supported in part by the Engineering Research Centers Program of the National Science Foundation under Award Number EEC-9986866. Subject Editor F. K. Forster.

S. McNamara was with the Department of Electrical Engineering and Computer Science, University of Michigan, Ann Arbor, MI 48109 USA. He is now with the Department of Electrical and Computer Engineering, University of Louisville, Louisville, KY 40292 USA (e-mail: shamus.mcnamara@louisville.edu).

Y. B. Gianchandani is with the Department of Electrical Engineering and Computer Science, University of Michigan, Ann Arbor, MI 48109 USA (e-mail: yogesh@umich.edu).

Digital Object Identifier 10.1109/JMEMS.2005.850718

[1]Portions of this paper appear in conference abstract form in [9], [10].

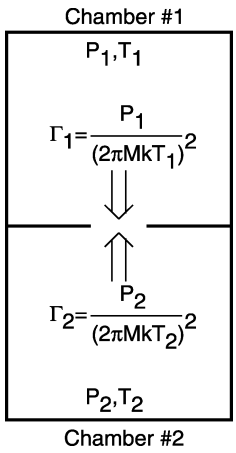

Fig. 1. The principle of thermal transpiration states that two chambers at differing temperatures generate a pressure differential due to differences in the rate of molecular flux from either chamber.

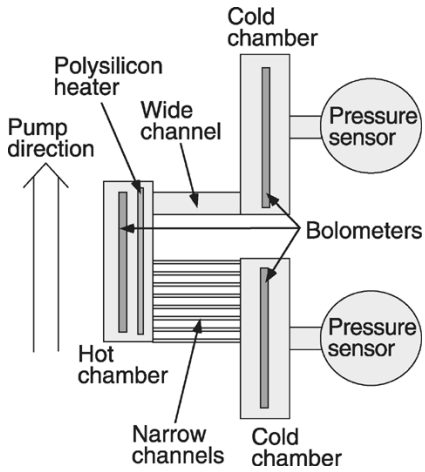

Fig. 2. Layout of a Knudsen pump showing two cold chambers, one hot chamber, the wide channel and parallel narrow channels. Attached to each cold chamber is a pressure sensor, and at the bottom of every chamber is a bolometer.

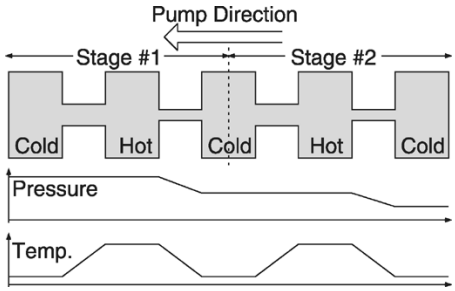

Fig. 3. Schematic showing the operation of an ideal Knudsen pump. The pressure decreases in the narrow channels because of thermal transpiration. In the wide channels, thermal transpiration does not take place and the pressure remains constant.

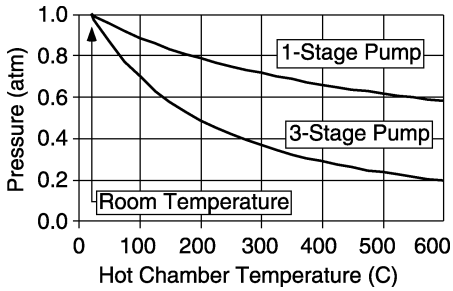

Fig. 4. Theoretical performance of the Knudsen pump as a function of hot chamber temperature and number of stages. To obtain this graph, the cold chamber is held constant at room temperature.

difference does not create a pressure difference between two volumes with a channel that permits viscous flow. The Knudsen pump (Fig. 2) creates a pressure increase from a cold region to a hot region through a very narrow channel in which the gas is in the free molecular flow regime. Then a wide channel is used to transport the gas in the viscous flow regime from the hot region to a second cold region. A lower pressure may be obtained by cascading multiple stages in series. The pressure ratio across the narrow channel may be derived by considering the ideal case of two adjacent chambers with an aperture separating them. One chamber is maintained at a "hot" temperature, the other chamber is "cold," and the gases are in the free molecular flow regime. The flux of gas molecules passing from one chamber to the other through the aperture is

$$\Gamma = \frac{n v_{\text{ave}}}{4} \tag{1}$$

where

$$n = \frac{P}{kT} \tag{2}$$

$$v_{\text{ave}} = \left(\frac{8kT}{\pi M}\right)^{\frac{1}{2}} \tag{3}$$

Γ is the flux of gas molecules going through the aperture, v_{ave} is the average velocity of the gas molecules, n is the gas number density, P is pressure, k is Boltzmann's constant, T is temperature, and M is the mass of a gas molecule. For steady-state operation the gas flux through the aperture in the two directions must be equal. With a little bit of algebra, the attainable pressure (P_{vac}) as a function of hot stage temperature (T_h), cold stage temperature (T_c), the outlet pressure (P_{outlet}), and the number of stages (s) is

$$P_{\text{vac}} = P_{\text{outlet}} \left(\frac{T_c}{T_h}\right)^{\frac{s}{2}}. \tag{4}$$

Although this derivation was performed for two volumes connected with an ideal aperture, the results are the same for two volumes connected with a channel.

Fig. 3 shows a schematic of the operation of an ideal Knudsen pump. The temperature profile shows that the hot chambers are at an elevated temperature and that the channels (wide and narrow) have a thermal gradient along their length. The pressure is constant except through a narrow channel, where thermal transpiration causes a pressure gradient. Fig. 4 shows the theoretical performance of a Knudsen pump operating with the cold chamber held at room temperature.

With regard to achieving the proper flow regime in the channels, it is helpful to use the Knudsen number as a guideline. The Knudsen number is defined as $Kn = \lambda/l$, where λ is the mean free path of the gas and l is the hydraulic diameter of the channel. Ideally, the narrow channels must have a hydraulic diameter less than 1/10 of the mean free path of the gas (i.e., for free molecular flow, $\text{Kn} > 10$) and the wide channels must have

a hydraulic diameter greater than 20 times the mean free path of the gas (i.e., for viscous flow $\mathrm{Kn} < 0.05$). However, both types of channels may be operated in the transition flow regime $(0.05 < \mathrm{Kn} < 10)$ with a possible loss of compression. Thus, the maximum operating pressure is increased by minimizing the hydraulic diameter of the narrow channels, whereas the lowest attainable pressure (best vacuum) is enhanced by maximizing the hydraulic diameter of the wide channels.

The theoretical analysis presented here is in a simplified form and applies only for gases that are in the free-molecular flow regime within the narrow channels. This analysis neglects many important factors, such as gas-gas collisions (especially important for transitional flow), the probability of a gas molecule passing through a channel, temperature gradients within the gas volumes, surface effects, etc. A more thorough discussion of the phenomena of thermal transpiration can be found in [18], and a more detailed analysis of the Knudsen pump, including an analysis of its performance in the transition regime, can be found in [19].

III. Experimental Device

A six-mask fabrication process is used to cofabricate the Knudsen pump and capacitive pressure sensors [9]. A Cr/Au mask is evaporated onto a Borofloat glass wafer and patterned. Recesses 10 μm deep are formed by a wet etch in $\mathrm{HF} : \mathrm{HNO_3} : \mathrm{H_2O}$ 7:3:10, which produces sloping sidewalls to facilitate metallization. These recesses define the hot and cold chambers, the capacitive pressure sensor cavity, and the wide channels [Fig. 5(a)]. Titanium is sputtered and patterned to define the bolometers and lower electrode of the capacitive pressure sensor at the bottom of the recess, but the titanium extends to the top of the glass substrate to permit electrical contact in a subsequent step [Fig. 5(b)]. A bare silicon wafer is coated with $\mathrm{SiO_2}$, $\mathrm{Si_3N_4}$, $\mathrm{SiO_2}$, and 100-nm -thick polysilicon. The polysilicon is patterned to define areas for lead transfer and to define the narrow channels [Fig. 5(c)]. An additional 900 nm of polysilicon is deposited, doped, and annealed, creating regions of polysilicon 900-nm thick and 1-μm thick. The full 1-μm-thick polysilicon is patterned to isolate regions defining the heater, the upper electrode of the capacitive pressure sensor, and regions for lead transfer [Fig. 5(d)]. The glass and silicon wafers are anodically bonded (through the polysilicon), creating sealed microcavities and connecting the titanium on the glass substrate to the polysilicon on the silicon substrate. The narrow channels are formed because the thinner polysilicon (900 nm) does not touch the glass substrate, leaving a 100-nm-thick channel. The entire silicon wafer is dissolved, leaving cavities sealed with dielectric/polysilicon diaphragms [Fig. 5(e)]. The substrate is also planar, permitting additional planar microfabrication techniques to be used and avoiding stress concentrations. The dielectric stack is selectively dry etched to form electrical vias for interconnect to the polysilicon and to create the polysilicon membranes for the pressure sensor [Fig. 5(f)]. Finally, titanium is deposited and patterned to define the top metal and bonding pads [Fig. 5(g)]. Fig. 5(g) is an expanded cross section of the final device, showing a hot chamber (left) connected to a cold chamber (middle) via a narrow channel, and a capacitive pressure sensor on the right. A suspended bonding pad to minimize parasitic capacitances is also shown adjacent to the pressure sensor.

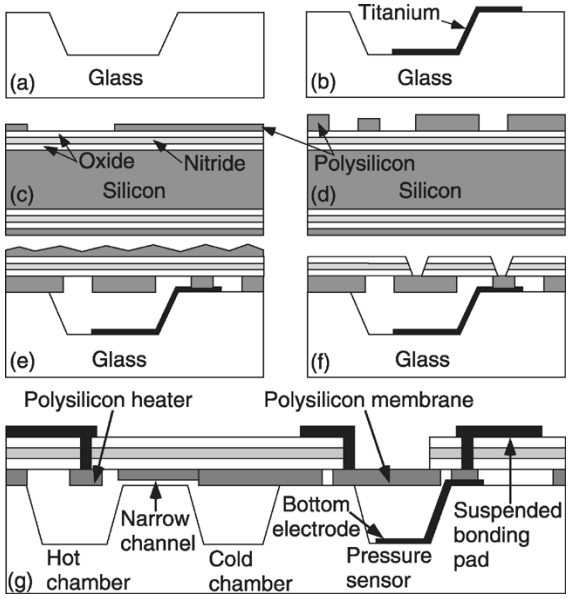

Fig. 5. (a)–(f) Fabrication steps used to create the Knudsen compressor and capacitive pressure sensors. (g) Final cross section of the Knudsen pump, drawn at a larger scale, showing hot and cold chambers connected by a narrow channel, and a capacitive pressure sensor used to measure the pump performance.

There are three levels of interconnect available in the finished device [Fig. 5(g)]: a top metal level, a suspended polysilicon layer, and a buried metal level. A dielectric layer separates the top metal and polysilicon. The polysilicon and buried metal are separated by an air gap. The dielectric cover is selected to maximize thermal isolation, provide a cover with a small gas permeation rate, and minimize parasitic capacitances.

The cold chambers are passively maintained at room temperature. A polysilicon heater located near the narrow channels heats the hot chamber. The heater is suspended on a thin dielectric membrane in order to minimize heat flow from the heater to the substrate. This technique has been demonstrated to achieve thermal isolation values greater than 1000 K/W [20]. A glass substrate is used to provide thermal insulation and, thereby, improve the energy efficiency. A long channel length is used to improve thermal isolation between the hot and cold chambers. Thin-film bolometers are located on the bottom of every chamber, allowing the temperature distribution and thermal isolation to be measured.

The wide channels are 10 μm deep and 30 μm wide. This ensures that the gas flow is in the viscous regime for pressures down to 300 torr with a hot chamber temperature of 600 °C. The narrow channels are 10-μm wide and 100-nm deep, corresponding to a Knudsen number of 0.6. This is in the transition regime to provide a higher gas flow rate while maintaining operation at atmospheric pressure. A long channel is used to reduce the thermal gradient along the channel and, hence, minimize power consumption, and multiple channels are used in parallel to increase the flow rate.

A capacitive pressure sensor [21], [22] is located adjacent to every cold chamber, as far away as possible from the hot

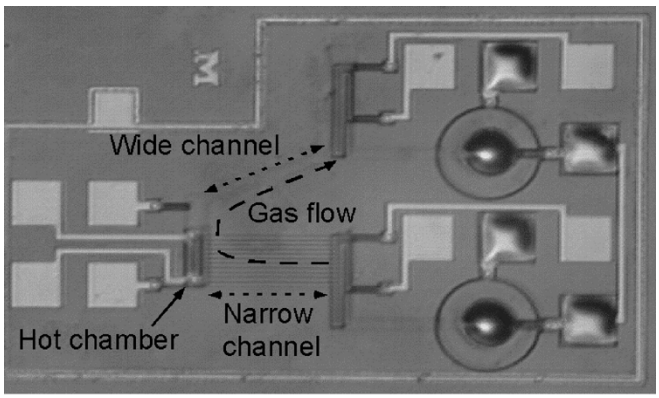

(a)

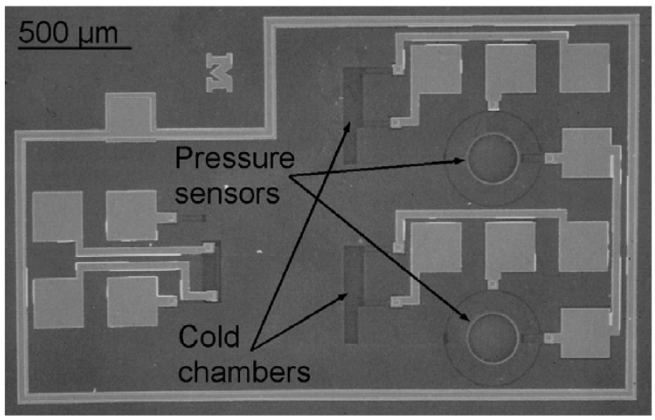

(b)

Fig. 6. (a) Optical micrograph. (b) SEM of a single stage pump prior to the formation of the pump outlet. The pump is sealed, causing the pressure sensor membranes to deflect in the optical micrograph because of the ambient pressure.

chamber to avoid unintended heating. The top electrode is a 1-μm-thick, 200-μm-diameter polysilicon membrane and the bottom titanium electrode is located at the bottom of a 10 μm recess in the glass. Due to its small size, the sensitivity of the pressure sensor is limited in part by parasitic capacitances. To alleviate this problem, the bonding pads are suspended on the dielectric layer over a 1-μm air gap over the glass substrate, eliminating all electrically conductive materials from the vicinity of the bonding pad. The bonding pads are sufficiently robust to permit testing and packaging.

IV. Measurement Results

Fig. 6 shows an optical micrograph and an SEM image of the same single-stage fabricated device before an outlet is formed for the pump [10]. At this time, the interior of the Knudsen pump is sealed under vacuum. The optical micrograph [Fig. 6(a)] shows deflected pressure sensor diaphragms due to the ambient pressure, but the SEM image [Fig. 6(b)] has flat diaphragms due to the vacuum ambient. Fig. 7 shows SEM images of the channel cross sections. The wide channel [Fig. 7(a)] is etched 10 μm into the glass and has a dielectric cover. The narrow channel [Fig. 7(b), (c)] is 10-μm wide but only 100-nm high. The figure shows that the polysilicon did not bond to the glass along the narrow channel despite the very small gap.

Fig. 8 shows an optical micrograph of a bonding pad that offers not only high thermal isolation but also very low parasitic

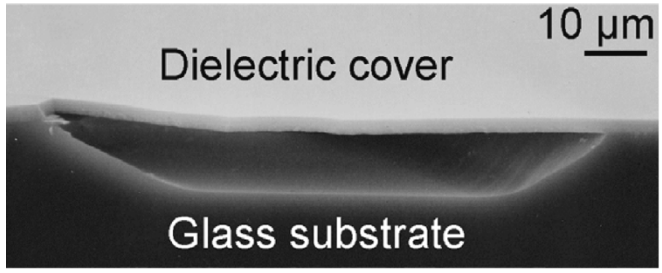

(a)

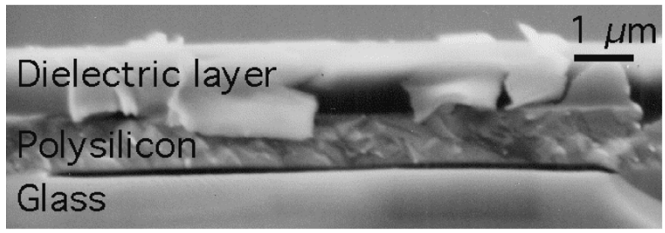

(b)

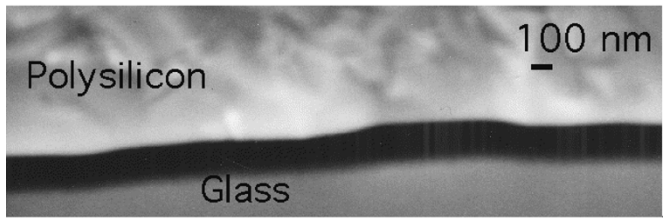

(c)

Fig. 7. SEM of channel cross sections. (a) A wide-channel 10-μm deep. (b) A narrow channel only 10-μm wide but only 100 nm in height. (c) A close-up of the narrow channel.

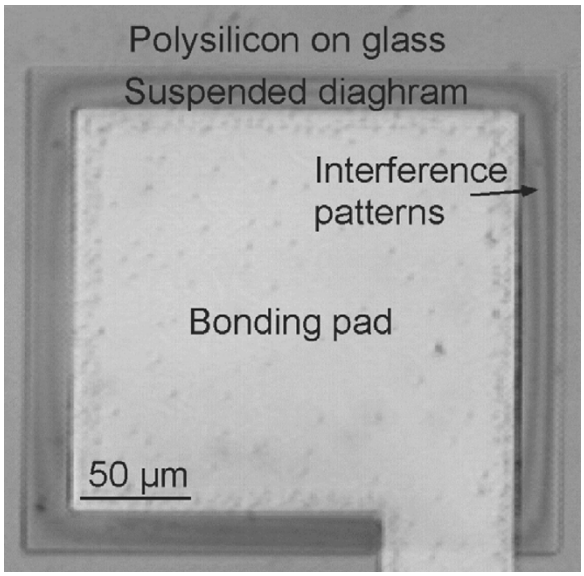

Fig. 8. Optical micrograph of a suspended bonding pad used to reduce parasitic capacitance. The bonding pad is deflected due to the ambient pressure, causing interference patterns to appear.

capacitance (measured at $<$1 fF) because it is suspended. The region under the bonding pad is sealed under vacuum, causing the observed deflection around the edges of the metal. Such features may make this fabrication process attractive for capacitive sensors and RF microsystems.

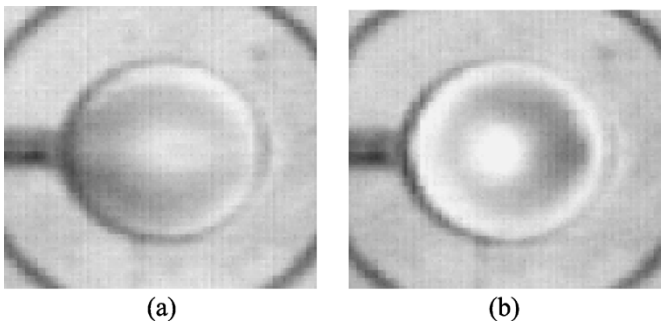

Fig. 9. Picture of a 200-μm-diameter pressure sensor (a) not deflected and (b) deflected when the pump was turned on. The measured capacitance change is 2.6 fF, corresponding to a cavity pressure of 0.46 atm.

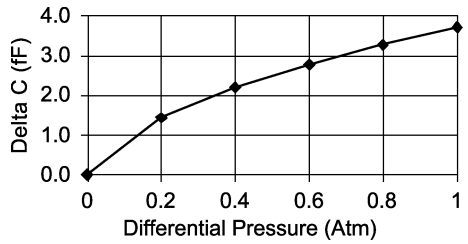

Fig. 10. ANSYS simulation of the capacitive pressure sensor response.

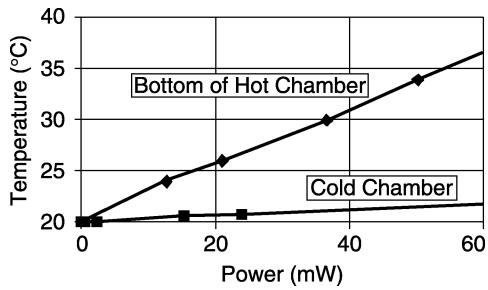

Fig. 11. The bolometers at the bottom of the hot and cold chambers show that the temperature increase is small across the die.

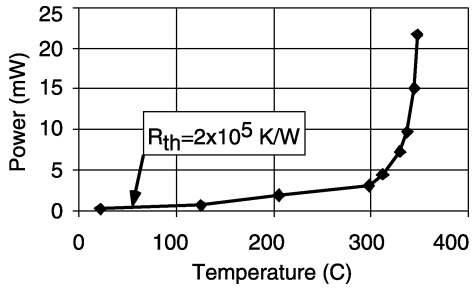

Fig. 12. Measured thermal isolation as a function of temperature of a 1-mm-long suspended polysilicon heater.

The operation of the Knudsen pump whose outlet is vented to atmosphere can be observed by watching the deflection of the vacuum cavity pressure sensor (Fig. 9). The pressure sensor membrane is flat with no power to the Knudsen pump [Fig. 9(a)], but it is deflected with the power on [Fig. 9(b)]. Finite-element analysis was performed using ANSYS to predict the response of the pressure sensor (Fig. 10). The measured change in capacitance is 2.6 fF, which corresponds to a cavity pressure of 0.46 atm. The input power is 80 mW and the calculated heater temperature from (4) is $\approx 1100\,^{\circ}\mathrm{C}$.

The pump speed can be estimated from the decay of the pressure as a function of time. The pump speed will decrease approximately linearly with respect to pressure, dropping to zero at the ultimate pressure. If outgassing from the chamber walls is neglected, the maximum pump speed can be estimated as

$$S = \frac{V}{2t} \ln \frac{P_i}{P_f} \tag{5}$$

where V is the volume, t is the pumpdown time, P_i is the initial pressure, and P_f is the final pressure. The factor of two occurs because of the pump speed decreases as the pressure drops. The visibly observed time to pump down is two seconds and the combined cold chamber, channel, and pressure sensor volume is 80 000 cubic micrometers. The estimated maximum pump speed is, therefore, 1×10^{-6} cc/min. By comparison, the estimated pump speed based on the analysis presented in [12] suggests that a pump speed of 3×10^{-5} cc/min can be achieved for the Knudsen pump presented in this paper. There are many possible reasons for this discrepancy, including measurement error (the pumpdown time could be much faster than was observed), the exclusion of outgassing in the analysis, errors in the hand-analysis because of the complex geometry and thermal distributions present in this Knudsen pump, or blockages in the narrow channels, to name a just a few. At 80 mW, the power required to operate at this flow rate is orders of magnitude greater than the results reported from a simulation for a related structure [11]. This discrepancy is in large part due to the parasitic heat losses to the substrate and ambient and illustrates the importance of good thermal management in the design of an efficient Knudsen pump.

Using embedded bolometers, the bottom of the hot chamber is measured to rise by $\approx 10\,^{\circ}\mathrm{C}$ with 35 mW of power to the polysilicon heater on the diaphragm above it, and a neighboring cold chamber rises $\approx 1\,^{\circ}\mathrm{C}$ (Fig. 11). The temperature coefficient of resistance (TCR) of the polysilicon was measured to be -1213 ppm over a range up to 100 °C. Assuming the TCR is constant over a much larger temperature range, the thermal isolation of a 1-mm-long suspended polysilicon heater was found to be approximately 2×10^5 K/W (Fig. 12). The thermal isolation of the Knudsen pump at 1100 °C (with a 250 μm long heater) is estimated to be 1.4×10^4 K/W. These thermal measurements prove that the pump should experience no loss of performance due to undesired heating of the cold chamber.

V. Conclusion

This effort demonstrates not only that a single chip Knudsen pump is feasible, but also that it can operate at atmospheric pressure. Atmospheric operation, which has been reported only once before, is made possible by taking advantage of the small feature sizes achievable in microfabrication without using aggressive lithography. A single stage pump and two integrated capacitive pressure sensors occupy an area 1.5 mm $\times$ 2 mm. The pressure in a microcavity is 0.46 atm at 80 mW of input power. Multiple stages may be cascaded in series to create a pump with a lower ultimate pressure.

The maximum pump speed is 1×10^{-6} cc/min. This flow rate is very small compared to conventional pumps, but it is

reasonable for an on-chip pump, as evidenced by the fact that it takes only two seconds to pump down.

The fabrication process developed has many features that make it applicable to other micromachined devices. The process is capable of creating narrow channels with a hydraulic diameter of less than 100 nm, making it suitable for gas and liquid devices that require a small hydraulic diameter, such as the electro-osmotic flow pump. The high thermal isolation that was obtained (as high as 2×10^5 K/W) is suitable for isolating other temperature-dependent sensors and actuators, such as convection-based flow meters or microhotplates, from their surroundings and minimizing their power consumption. The suspended bonding pads are ideally suited for all devices that use capacitive-based sensors because the parasitic capacitances are very small (<1 fF). Electrical lead-transfer with low parasitic resistance ($< 1\ \Omega$) and capacitance (<1 fF) may be made to the interior of a vacuum-encapsulated cavity using this process. Finally, the 6-mask process is silicon IC-compatible because only polysilicon, Si-dielectric materials, metal, and glass are needed.

Although the Knudsen pump was used to evacuate a cavity in this effort, the larger goal was the demonstration of the concept. It may be used for gas sampling applications, pneumatic actuation, and vacuum encapsulation.

ACKNOWLEDGMENT

The facilities used for this research include the Solid-State Electronics Laboratory (SSEL) at the University of Michigan. The authors wish to thank Prof. J. Pfofenhauer at the University of Wisconsin for encouraging us to work on this topic.

REFERENCES

[1] R. A. Miller, E. G. Nazarov, G. A. Eiceman, and A. T. King, "A MEMS radio-frequency ion mobility spectrometer for chemical vapor detection," *Sens. Actuators*, vol. A91, p. 301, 2001.

[2] C. Wilson and Y. B. Gianchandani, "Silicon micro-machining using in-situ DC microplasmas," *J. Microelectromech. Syst.*, vol. 10, no. 1, p. 50, 2001.

[3] F. Iza and J. Hopwood, "Influence of operating frequency and coupling coefficient on the efficiency of microfabricated inductively coupled plasma sources," *Plasma Sources Sci. Technol.*, vol. 11, p. 1, 2002.

[4] C. G. Wilson and Y. B. Gianchandani, "Spectral detection of metal contaminants in water using an on-chip microglow discharge," *IEEE Trans. Electron Devices*, vol. 49, no. 12, pp. 2317–2322, 2002.

[5] J. P. Hobson and D. B. Salzman, "Review of pumping by thermal molecular pressure," *J. Vac. Sci. Technol.*, vol. A18, no. 4, p. 1758, 2000.

[6] M. Knudsen, *Annals Der Physik*, 1910, vol. 31, p. 205.

[7] J. P. Hobson, "Accommodation pumping—a new principle," *J. Vac. Sci. Technol.*, vol. 7, no. 2, p. 351, 1970.

[8] D. H. Tracey, "Thermomolecular pumping effect," *J. Phys. E: Sci. Instr.*, vol. 7, p. 533, 1974.

[9] S. McNamara and Y. B. Gianchandani, "A fabrication process with high thermal isolation and vacuum sealed lead transfer for gas reactors and sampling microsystems," in *Proc. IEEE 16th Annual Int. Conf. Micro Electromech. Syst.*, 2003, pp. 646–649.

[10] ——, "A micromachined Knudsen pump for on-chip vacuum," in *Dig. Tech. Papers 12th Int. Conf. Solid-State Sensors and Actuators*, 2003, pp. 1919–1922.

[11] E. P. Muntz and S. E. Vargo, "Microscale vacuum pumps," in *The MEMS Handbook*, M. Gad-el-Hak, Ed. Boca Raton, FL: CRC, 2002, ch. 29.

[12] D. J. Turner, "A mathematical analysis of a thermal transpiration vacuum pump," *Vacuum*, vol. 16, no. 8, p. 413, 1966.

[13] C. C. Wong, M. L. Hudson, D. L. Potter, and T. J. Bartel, "Gas transport by thermal transpiration in micro-channels—a numerical study," in *Proc. ASME MEMS Conf.*, vol. DSC-66, Anaheim, CA, 1998, pp. 223–228.

[14] R. M. Young, "Analysis of a micromachine based vacuum pump on a chip actuated by the thermal transpiration effect," *J. Vac. Sci. Technol.*, vol. B17, no. 2, p. 280, 1999.

[15] S. E. Vargo, E. P. Muntz, and G. R. Shiflett, "Knudsen compressor as a micro- and macroscale vacuum pump without moving parts or fluids," *J. Vac. Sci. Technol.*, vol. A17, no. 4, p. 2308, 1999.

[16] S. E. Vargo and E. P. Muntz, "Initial results from the first MEMS fabricated thermal transpiration-driven vacuum pump," in *Rarefied Gas Dynamics: 22nd Int. Symp.*, 2001, p. 502.

[17] E. Kennard, *Kinetic Theory of Gases*. New York: McGraw Hill, 1938.

[18] S. C. Liang, "On the calculation of thermal transpiration," *J. Phys. Chem.*, vol. 57, p. 910, 1953.

[19] E. P. Muntz, Y. Sone, K. Aoki, S. Vargo, and M. Young, "Performance analysis and optimization considerations for a Knudsen compressor in transitional flow," *J. Vac. Sci. Technol. A*, vol. 20, no. 1, p. 214, 2002.

[20] N. Najafi, K. D. Wise, and J. W. Schwank, "A micromachined ultra-thin-film gas detector," *IEEE Trans. Electron Devices*, vol. 41, no. 10, p. 1770, 1994.

[21] J.-S. Park and Y. B. Gianchandani, "A servo-controlled capacitive pressure sensor using a capped-cylinder structure microfabricated by a three-mask process," *J. Microelectromech. Syst.*, vol. 12, no. 2, p. 209, 2003.

[22] J. Ji, S. T. Cho, Y. Zhang, K. Najafi, and K. D. Wise, "An ultracompliant CMOS pressure sensor for a multiplexed cardiovascular catheter," *IEEE Trans. Electron Devices*, vol. 39, no. 10, p. 2260, 1992.

Shamus McNamara (M'02) received the B.S. and M.S. degrees in electrical engineering from Rensselaer Polytechnic Institute in 1994 and 1996, respectively, and the Ph.D. degree, also in electrical engineering, from the University of Wisconsin, Madison, in 2002.

He was an Adjunct Lecturer with the Electrical Engineering and Computer Science Department, University of Michigan, Ann Arbor, during fall 2002 semester. From 2002 to 2004, he was a Research Fellow at the University of Michigan. He is currently an Assistant Professor with the Department of Electrical and Computer Engineering at the University of Louisville. His current research interests are in the design and fabrication of microsystems.

Yogesh B. Gianchandani (S'83–M'85–SM'04) received the B.S., M.S., and after some time in industry, the Ph.D. degrees in electrical engineering, with a focus on microelectronics and MEMS.

He is presently an Associate Professor with the Electrical Engineering and Computer Science Department, University of Michigan, Ann Arbor. Prior to this, he was with the Electrical and Computer Engineering Department, University of Wisconsin, Madison. He has also held industry positions with Xerox Corporation, Microchip Technology, and other companies, working in the area of integrated circuit design. His research interests include all aspects of design, fabrication, and packaging of micromachined sensors and actuators and their interface circuits. He has published about 130 papers in the field of MEMS and has about 20 patents issued or pending.

Prof. Gianchandani is the recipient of a National Science Foundation Career Award. He serves on the editorial boards of *Sensors and Actuators*, the *IOP Journal of Micromechanics and Microengineering*, and the *Journal of Semiconductor Technology and Science*. He also served on the steering and technical program committees for the IEEE/ASME International Conference on Micro Electro Mechanical Systems (MEMS) for many years, and served as a General Co-Chair for this meeting in 2002. At the University of Michigan, he serves as the Director of the College of Engineering Interdisciplinary Professional Degree Program in Integrated Microsystems.